Global Nonlinear Electromagnetic Simulations of Tokamak Turbulence

Alberto Bottino, Bruce Scott, Stephan Brunner, Ben F. McMillan, Trach Minh Tran, Thibaut Vernay, Laurent Villard, Sebastien Jolliet, Roman Hatzky, and Arthur G. Peeters

***Abstract*—The particle-in-cell code ORB5 is a global gyrokinetic turbulence simulation code in tokamak geometry. It has been developed at CRPP, Lausanne, Switzerland, with major contributions from IPP, Garching, Germany, and IPP, Greifswald, Germany, under a long-standing collaboration. The code ORB5 solves the gyrokinetic equations in the whole plasma core, including the magnetic axis. A field-aligned filtering procedure and sophisticated noise-control and heating operators allow for accurate simulations. Recently, the code ORB5 has been extended to include self-consistent perpendicular magnetic field perturbations. The inclusion of magnetic perturbations allows for a comprehensive study of finite β effects on microinstability. In this paper, we present the first linear and nonlinear code results concerning electromagnetic effects on tokamak microinstabilities.**

***Index Terms*—Particle-in-cell methods, plasma confinement, plasma stability, tokamaks.**

I. Introduction

PARTICLE-IN-CELL (PIC) methods have been widely used for solving the gyrokinetic equations and simulating turbulence in tokamaks and stellarators (see, for example, [1]–[3]). Most of the existing gyrokinetic PIC codes are based on the δf method [3], [4]. In the δf method, the distribution function f of each plasma species is split into a time-independent background distribution function f_0 and a time-dependent perturbation δf, $f = f_0 + \delta f$. In the δf method, only the perturbed part (δf) is discretized using numerical particles, also called markers. As long as the perturbation δf remains small as compared to f_0, the δf method reduces the statistical noise. The δf method can be interpreted as a "control variate" algorithm [5], [6], a variance reduction technique widely used in Monte Carlo methods. Many linear and nonlinear global gyrokinetic δf PIC codes exist and are routinely used for simulating electrostatic perturbations. However, the electrostatic approximation is expected to break down in the core of high β_e ($\beta_e \equiv \mu_0 n_e T_e / B^2$) plasmas or in any region where pressure gradients are large. For a finite value of β_e, the magnetic fluctuations modify the evolution of the electrostatic instabilities and eventually introduce new electromagnetic (EM) modes [7]. Therefore, a complete EM treatment of the plasma instabilities is desirable and must be included in the models and codes. EM simulations using a conventional δf method are much more demanding with respect to numerical resources than electrostatic simulations. In particular, the parallel electron dynamics imposes a strong constraint on the size of the time step. In addition to this, the EM simulations require a much larger number of numerical particles in order to describe correctly the evolution of the nonadiabatic part of the electron distribution function. Indeed, the physically relevant nonadiabatic part of the electron distribution function is overwhelmed by the adiabatic response to the magnetic potential $A_\parallel$ leading to a severe accuracy problem, known in the literature as the "cancellation problem" (see [6] and references therein). An accurate enough description of this small signal requires a very low statistical noise or, in other words, a huge number of numerical particles. Two main methods have been proposed to overcome this difficulty: the so called "split-weight" scheme, originally proposed in [8], and the use of an appropriate adjustable control variate method in a conventional δf scheme [6]. In particular, the control variate method reduces, by almost two orders of magnitudes, the number of numerical particles required for solving the cancellation problem [6]. The adjustable control variate method has been successfully applied in linear EM tokamak simulations [9]. In this paper, we show that the same method can also be applied to nonlinear simulations.

The code used in this paper is the global δf PIC code ORB5 [10]. The ORB5 solves the set of gyrokinetic equations in the whole plasma core down to the magnetic axis. The use of MHD equilibria leads to a consistent inclusion of geometrical parameters, such as the Shafranov shift, and allows for simulating most of the existing tokamak experiments and future reactor-size machines. A field-aligned filtering procedure and sophisticated noise-control and heating operators allow for accurate simulations with smaller numbers of markers than the standard δf PIC simulations [11]. The code ORB5 has been proven to scale up to 32 thousand cores on a BlueGene/P architecture. The strong scaling for the standard Cyclone base case, described in [12], is shown in Fig. 1. Note that this particular case has been selected as a reference benchmark case for global

Manuscript received December 1, 2009; revised May 1, 2010; accepted June 18, 2010. Date of publication August 3, 2010; date of current version September 10, 2010.

A. Bottino and B. Scott are with the Max-Planck-Institut für Plasmaphysik, IPP-EURATOM Association, 85748 Garching, Germany.

S. Brunner, B. F. McMillan, T. M. Tran, T. Vernay, and L. Villard are with the Centre de Recherches en Physique des Plasmas, Association EURATOM—Confédération Suisse, Ecole Polytechnique Fédérale de Lausanne, 1015 Lausanne, Switzerland.

S. Jolliet is with the Japan Atomic Energy Agency, Tokyo 110-0015, Japan.

R. Hatzky is with the Computer Center of the Max-Planck-Gesellschaft, 85748 Garching, Germany.

A. G. Peeters was with the Centre for Fusion, Space, and Astrophysics, University of Warwick, CV4 7AL Coventry, U.K. He is now with the University of Bayreuth, 95440 Bayreuth, Germany.

Color versions of one or more of the figures in this paper are available online at http://ieeexplore.ieee.org.

Digital Object Identifier 10.1109/TPS.2010.2055583

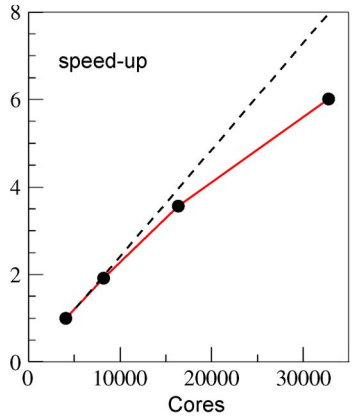

Fig. 1. Electrostatic ORB5: Strong scaling. Relative speedup from 4096 up to 32 768 cores for the Cyclone base case [12]; grid size of (128, 512, 256); 3×10^9 markers. Simulations performed on BlueGene/P, in collaboration with RZG Garching.

simulations by the EFDA Integrated Tokamak Modelling task force on instabilities and transport (IMP4) [13]. The Cyclone base case is based on the parameters of an existing experiment, the DIII-D tokamak in San Diego, USA. The grid size used in these simulations is (128, 512, 256) (for radial, poloidal, and toroidal directions, respectively), and the distribution function has been discretized by using 3×10^9 markers. The code shows a parallel efficiency of more than 75% at 32 thousand cores. The recent ORB5 simulations made on the IBM POWER6 and IBM BlueGene/P supercomputers showed that the inclusion of Ampère's law does not degrade the scaling properties of the ORB5 since the field solver time remains a small fraction of the total computational time.

The organization of this paper is as follows. In Section II, the gyrokinetic model used in the ORB5 is presented. Section III is dedicated to the discussion of the numerical implementation of the model focusing particularly on the problems related with the discretization of the field equations, particularly the cancellation problem. The simulation results are presented in Section IV.

II. Model

The code ORB5 is based on the gyrokinetic Vlasov-Maxwell system of equations of Hahm *et al.* [14], [15] and Brizard [16]. The latter consists of a set of self-consistent and energy-conserving nonlinear gyrokinetic equations for the particles and fields. Those equations are particularly suitable for the PIC simulations. They have the desirable feature that the polarization drift appears in the gyrokinetic Poisson equation and not in the gyro-averaged Vlasov equation. The full derivation of the equations using the Hamiltonian formalism and the Lie transforms can be found in [14] and [16]. In this paper, we report the final version of the gyrokinetic equations as they are implemented in the ORB5. The time evolution of the particle distribution function F_s, for a plasma species s, is determined by the gyro-averaged Vlasov equation

$$\frac{dF_s}{dt} = \frac{\partial F_s}{\partial t} + \frac{\partial F_S}{\partial \mathbf{R}} \cdot \dot{\mathbf{R}} + \frac{\partial F_s}{\partial p_\parallel} \dot{p}_\parallel = 0. \tag{1}$$

The characteristics are given by

$$\begin{aligned} \frac{d\mathbf{R}}{dt} = & \left(p_\parallel - \frac{q_i}{m_i}\langle A_\parallel \rangle_s\right)\mathbf{h} + \frac{1}{\Omega_i B_\parallel^*}\left(p_\parallel^2 + \mu B\right) \\ & \times (\mathbf{h}\times\nabla B) - \frac{p_\parallel^2}{\Omega_i B_\parallel^*}\mathbf{h}\times[\mathbf{h}\times(\nabla\times\mathbf{B})] + \frac{\mathbf{B}\times\nabla\langle\Psi\rangle_s}{B_\parallel^* B} \\ & - \langle A_\parallel\rangle_s p_\parallel \left\{\mathbf{h}\times\frac{\nabla B}{B} - \mathbf{h}\times\left[\mathbf{h}\times\left(\frac{\nabla\times\mathbf{B}}{B}\right)\right]\right\} \end{aligned} \tag{2}$$

$$\begin{aligned} \frac{dp_\parallel}{dt} = & -\mu\nabla\mathbf{B}\cdot\mathbf{h} - \nabla\langle\Psi\rangle_s \\ & \times\left\{\frac{q_i}{m_i}\mathbf{h} + \frac{p_\parallel}{BB_\parallel^*}(\mathbf{h}\times\nabla B) - \frac{p_\parallel}{BB_\parallel^*}\mathbf{h}\times[\mathbf{h}\times(\nabla\times B)]\right\} \end{aligned} \tag{3}$$

$$B_\parallel^* \equiv \mathbf{B}\cdot\mathbf{h} + \frac{m_s p_\parallel}{q_s}(\nabla\times\mathbf{h})\cdot\mathbf{h}, \qquad \mathbf{h} \equiv \frac{\mathbf{B}}{B} \tag{4}$$

where $\mathbf{R}$, $p_\parallel$, and μ are the gyrocenter position, the parallel momentum per unit mass, and the magnetic moment per unit mass, $\mu \equiv v_\perp^2/2B$, respectively. $B_\parallel^*$ is the phase-space Jacobian of the gyrocenter phase-space while $\langle\rangle_s$ indicates the gyro-averaged quantities. As compared to the original gyrokinetic equations, the second-order terms in the component of the magnetic potential parallel to the magnetic field, $A_\parallel$, are neglected in both the generalized momentum and the gyro-averaged effective potential $\langle\Psi\rangle_s$

$$\langle\Psi\rangle_s \equiv \langle\phi\rangle_s - p_\parallel\langle A_\parallel\rangle_s. \tag{5}$$

The self-consistent gyrokinetic field equations are given by the parallel component of the gyrokinetic Ampère's law

$$\frac{\beta_i}{\rho_i^2}A_\parallel + \frac{\beta_e}{\rho_e^2}A_\parallel - \nabla_\perp\cdot\left[(1-\beta_i)\nabla_\perp A_\parallel\right] = \mu_0\left(\langle j_{\parallel,i}\rangle + j_{\parallel,e}\right) \tag{6}$$

and the gyrokinetic Poisson equation (quasi-neutrality) for the electrostatic potential ϕ

$$-\nabla_\perp\cdot\left(\frac{Z_i n_0}{B\Omega_i}\nabla_\perp\phi\right) = \langle n_i\rangle - n_e \tag{7}$$

where ρ_s is the thermal gyroradius and $\beta_s \equiv \mu_0 n_s T_s/B_0^2$ of the species s. The two previous equations have been written under the assumption of an equilibrium Maxwellian distribution function f_{0s} of density n_{0s} and considering the electrons and main ions only ($n_{0s} \equiv n_{0i} = n_{0e}$). Moreover, the field equations (6) and (7) have been obtained by applying the so-called long-wavelength approximation ($O(k_\perp\rho_i)^2$) and the drift-kinetic approximation for the electrons to the original equations of [16].

The particle and current densities, $\langle n_s\rangle$ and $\langle j_{\parallel s}\rangle$, are

$$\begin{aligned} \langle n_s\rangle(\mathbf{x}) &\equiv \int F_s(\mathbf{R}, p_\parallel, \mu)\delta(\mathbf{R} + \boldsymbol{\rho_s} - \mathbf{x})d^6Z \\ \langle j_{\parallel s}\rangle(\mathbf{x}) &\equiv \int p_\parallel F_s(\mathbf{R}, p_\parallel, \mu)\delta(\mathbf{R} + \boldsymbol{\rho_s} - \mathbf{x})d^6Z. \end{aligned} \tag{8}$$

The code ORB5 solves the particle and field equations in magnetic coordinates, (s, θ_*, φ)

$$s \equiv \sqrt{\frac{\psi}{\psi_{\rm edge}}} \tag{9}$$

where ψ is the poloidal magnetic flux and

$$\theta_* \equiv \frac{1}{q(\psi)} \int_0^\theta \frac{\mathbf{B}\cdot\nabla\varphi}{\mathbf{B}\cdot\nabla\theta'} d\theta' \tag{10}$$

θ, and φ are the poloidal and toroidal angles, respectively.

The Jacobian $J_*^{-1} = \nabla\theta_* \cdot (\nabla\psi \times \nabla\varphi)$ is given by

$$J_* = J\frac{\partial\theta}{\partial\theta_*} = \frac{R^2 q(\psi)}{F(\psi)} \tag{11}$$

where $J^{-1} = \nabla\theta \cdot (\nabla\psi \times \nabla\varphi)$. The poloidal and magnetic angle coordinates are related by

$$\frac{\partial\theta_*}{\partial\theta} = \frac{1}{q(\psi)}\frac{\mathbf{B}\cdot\nabla\varphi}{\mathbf{B}\cdot\nabla\theta'} = \frac{F(\psi)J}{q(\psi)R^2} \tag{12}$$

where q is the safety factor.

The magnetic field is defined as

$$\mathbf{B} = F(\psi)\nabla\varphi + \nabla\psi \times \nabla\varphi \tag{13}$$

where $F(\psi)$ is the poloidal current flux function.

A detailed description of the implementation of the ORB5 equations in the magnetic coordinates in the electrostatic limit is given in [10].

In the EM case, the equations of motion solved by the ORB5 in the magnetic coordinates are

$$\begin{aligned}\frac{ds}{dt} =& \frac{m_i\left(p_\parallel^2 + B\mu\right)}{q_i B_\parallel^* B^2 J_{*s}} F\frac{\partial B}{\partial\theta_*} - \nabla_\varphi\langle\Psi\rangle\frac{\nabla\psi\cdot\nabla\mathbf{s}}{R^2 B B_\parallel^*} \\ &+ \nabla_{\theta_*}\langle\Psi\rangle\frac{F}{J_{*s}BB_\parallel^*} - \langle A_\parallel\rangle p_\parallel\frac{F}{J_{*s}B^2}\frac{\partial B}{\partial\theta_*}\end{aligned} \tag{14}$$

$$\begin{aligned}\frac{d\theta_*}{dt} =& \frac{p_\parallel}{J_{*\psi}B} - \frac{m_i\left(p_\parallel^2 + B\mu\right)}{q_i B_\parallel^* B^2 J_{*s}} F\frac{\partial B}{\partial s} - \frac{m_i p_\parallel^2 p' F}{q_i B_\parallel^* B^3 J_{*\psi}} \\ &- \nabla_\varphi\langle\Psi\rangle\frac{\nabla\psi\cdot\nabla\theta_*}{R^2 B B_\parallel^*} - \nabla_s\langle\Psi\rangle\frac{F}{J_{*s}BB_\parallel^*} \\ &- \langle A_\parallel\rangle\left[\frac{q_i}{m_i}\frac{1}{BJ_{*\psi}} + \frac{p_\parallel}{B^2}\left(\frac{F}{J_{*s}}\frac{\partial B}{\partial s} + \frac{Fp'}{J_{*\psi}B}\right)\right]\end{aligned} \tag{15}$$

$$\begin{aligned}\frac{d\varphi}{dt} =& \frac{p_\parallel F}{BR^2} + \frac{m_i\left(p_\parallel^2 + B\mu\right)}{q_i B_\parallel^* B^2 R^2} \\ &\times\left(\frac{\partial B}{\partial s}\nabla\psi\cdot\nabla s + \frac{\partial B}{\partial\theta_*}\nabla\psi\cdot\nabla\theta_*\right) + \frac{m_i p_\parallel^2 p'|\nabla\psi|^2}{q_i B_\parallel^* B^3 R^2} \\ &+ \nabla_s\langle\Psi\rangle\frac{\nabla\psi\cdot\nabla\mathbf{s}}{R^2 B B_\parallel^*} + \nabla_{\theta_*}\langle\Psi\rangle\frac{\nabla\psi\cdot\nabla\theta_*}{R^2 B B_\parallel^*} \\ &- \langle A_\parallel\rangle\left[\frac{q_i F}{m_i B R^2} + \frac{p_\parallel}{B^2 R^2}\right. \\ &\times\left(\frac{\partial B}{\partial s}\nabla\psi\cdot\nabla s + \frac{\partial B}{\partial\theta_*}\nabla\psi\cdot\nabla\theta_*\right) \\ &\left.+\frac{p_\parallel p'}{R^2 B^3}|\nabla\psi|^2\right]\end{aligned} \tag{16}$$

$$\begin{aligned}\frac{dp_\parallel}{dt} =& -\frac{\mu}{BJ_{*s}}\frac{\partial B}{\partial\theta_*} - \nabla_s\langle\Psi\rangle\frac{p_\parallel}{B_\parallel^*}\frac{F}{B^2 J_{*s}}\frac{\partial B}{\partial\theta_*} - \nabla_{\theta_*}\langle\Psi\rangle \\ &\times\left(\frac{q_i}{m_i}\frac{1}{J_{*\psi}B} - \frac{p_\parallel}{B_\parallel^*}\frac{F}{B^2 J_{*s}}\frac{\partial B}{\partial s} - \frac{p_\parallel}{B_\parallel^*}\frac{p'F}{B^3 J_{*\psi}}\right) \\ &- \nabla_\varphi\langle\Psi\rangle\left(\frac{q_i}{m_i}\frac{F}{R^2 B} + \frac{p_\parallel}{B_\parallel^*}\right. \\ &\times\left[\frac{\partial B}{\partial s}\nabla s\cdot\nabla\psi + \frac{\partial B}{\partial\theta_*}\nabla\psi\cdot\nabla\theta_*\right] \\ &\left.\times\frac{1}{B^2R^2} + \frac{p_\parallel}{B_\parallel^*}\frac{p'|\nabla\psi|^2}{B^3R^2}\right)\end{aligned} \tag{17}$$

where $J_{*\psi} \equiv (\nabla\theta_* \times \nabla\psi)\cdot\nabla\varphi)^{-1}$ and $J_{*s} \equiv (\nabla\theta_* \times \nabla s)\cdot\nabla\varphi)^{-1}$. The definition of p' appearing in the previous equations depends on the type of equilibrium chosen. Two kinds of magnetic equilibria are implemented in the ORB5: the circular concentric flux surfaces, referred to as the *ad hoc* equilibrium in [10], and the true MHD equilibrium solution of the Grad-Shafranov equation. For the latter case, the ORB5 is coupled to the fixed-boundary equilibrium code CHEASE [17]. For the MHD equilibria, p' is the first derivative of the pressure profile in ψ while for the *ad hoc* equilibria

$$\begin{aligned}p'(\psi) =& -\frac{g(\psi)}{R^2} \\ g(\psi) \equiv& \nabla^2\psi - \frac{2}{R}\frac{\partial\psi}{\partial R}.\end{aligned}$$

III. Numerical Implementation

A detailed description of the numerical implementation of the model equations in the electrostatic approximation is given in [10]. In this paper, we just remind that the Vlasov equation for the perturbed distribution function δf_s is solved using the PIC method: δf_s is discretized with a finite number N of numerical particles or markers. Each marker p is defined by a weight w_p and a position $(\mathbf{R}_p, p_{\parallel p}, \mu_p)$ in the 5-D phase space of the gyrocenters

$$\begin{aligned}\delta f_s =& \frac{N_{\rm ph}}{N}\sum_{p=1}^{N}\frac{1}{2\pi B_\parallel^*} w_p(t)\delta\left(\mathbf{R} - \mathbf{R}_p(t)\right) \\ &\times\delta\left(p_\parallel - p_{\parallel,p}(t)\right)\delta\left(\mu - \mu_p(t_0)\right)\end{aligned} \tag{18}$$

where $N_{\rm ph}$ is the total number of physical particles.

Inserting the previous equation into the gyrokinetic Vlasov equation (1) and integrating on a volume Ω_p on which δf_s is

assumed to be a constant, we obtain an evolution equation for each single weight w_p. The resulting equation and the particle trajectory equations (14:17) are integrated in time for each numerical particle using a Runge–Kutta integrator of order four.

The field equations are discretized using B-spline finite elements

$$\phi(\mathbf{x},t) = \sum_{\mu} \phi_{\mu}(t)\Lambda_{\mu}(\mathbf{x})$$

$$A_{\parallel}(\mathbf{x},t) = \sum_{\mu} A_{\parallel,\mu}(t)\Lambda_{\mu}(\mathbf{x})$$

where μ stands for (i,j,k) on the three spatial components and Λ_{μ} denote the tensor products of the 1-D B-splines (see, for example, [18]). Note that all the simulations presented in this paper have been computed using cubic B-splines.

Ampère's law is discretized and solved using the same algorithm described in [10] for the Poisson equation.

In addition to the introduction of Ampère's law and the inclusion of $A_{\parallel}$ in the particle equations, the main modifications to the algorithms of the ORB5 code are related to the so-called cancellation problem (see, for example, [6]). In the $p_{\parallel}$ formulation, the adiabatic component of the current $\langle j_{\parallel s}\rangle^{\mathrm{ad}} \equiv \langle j_{\parallel s}\rangle - \langle j_{\parallel s}\rangle^{\mathrm{nonad}}$ cancels exactly the skin term $\beta_s/\rho_s^2 A_{\parallel}$ on the left-hand side of (6). Accordingly, only the nonadiabatic current represents a physically relevant quantity. This imposes a severe constraint on the required accuracy for the discretization of Ampère's law equation. Indeed, the numerically discretized current (using numerical particles) has to represent both the adiabatic and nonadiabatic parts. The nonadiabatic part is, in general, a small fraction of the total current and can easily be swamped by discretization errors associated with the finite number of markers used in the simulations.

The cancellation problem of the unphysical adiabatic currents is solved using an adjustable control variate method proposed in [6]. The control variate used to reduce the numerical error corresponds, in this case, to the part of the distribution function of the electrons responding adiabatically to the magnetic potential $A_{\parallel}$. This scheme is described in detail in [6, Sec. 8.2]. Note that the same scheme has been successfully applied in the linear PIC simulations in tokamak geometry [19].

In addition to this, the field equations have been modified in the following way

$$\begin{aligned} C_A\left(\frac{\beta_i}{\rho_i^2}+\frac{\beta_e}{\rho_e^2}\right)A_{\parallel} - \nabla_{\perp}\cdot\left[(1-\beta_i)\nabla_{\perp}A_{\parallel}\right] \\ = \mu_0\left(\langle j_{\parallel,i}\rangle + j_{\parallel,e}\right) - C_q\nabla_{\perp}\cdot\left(\frac{en_0}{k_B\Omega_i}\nabla_{\perp}\phi\right) \\ = \langle n_i\rangle - n_e \end{aligned}$$

where C_A and C_q take into account the finite extent of the velocity space domain in the simulation. The value of C_A is close to unity and varies with the radius. The inclusion of this factor is crucial for the correct solution of the cancellation problem [9].

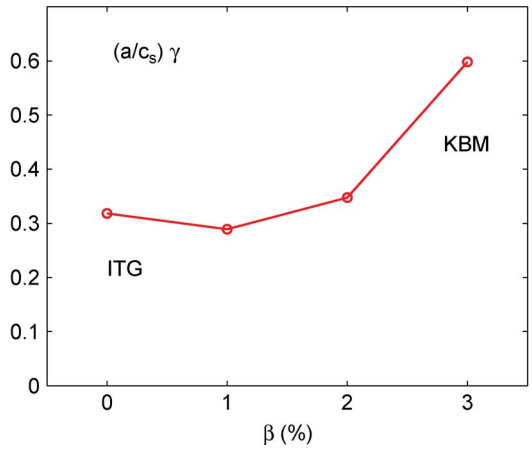

Fig. 2. Linear growth rate as a function of β_e in tokamak geometry; circular cross section $\rho^* \simeq 1/55$.

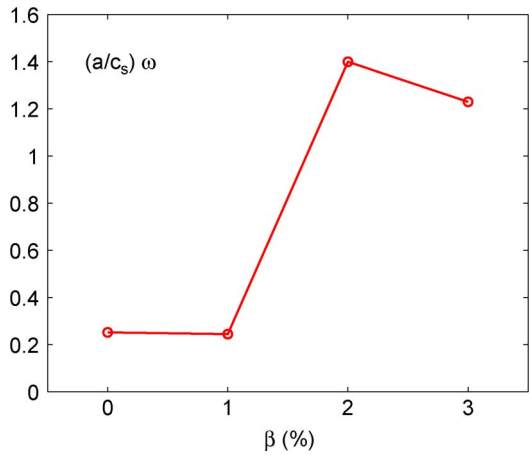

Fig. 3. Real frequency as a function of β_e in tokamak geometry, $\rho^* = 1/55$. Positive sign corresponds to the ion diamagnetic direction.

IV. Simulation Results

The EM version of the ORB5 has been tested and benchmarked against the linear EM code GYGLES (see [19] and references therein) in a simpler cylindrical geometry. In this paper, we report the first linear and nonlinear results in the tokamak geometry. Figs. 2 and 3 show the growth rate and the real part of the frequency of the most unstable mode for different values of β_e for a tokamak equilibrium. For these simulations, we have used a circular *ad hoc* equilibrium with major radius $R_0 = 2.0$ m, minor radius $a = 0.5$ m, and $\rho^* \equiv \rho_s/a \simeq 1/55$ at midradius. The value of the density on the axis has been varied in the simulations in order to perform a scan in β_e. The background profiles have been chosen to give $R/L_{Te} \equiv R/L_{Ti} \simeq 10$ at $r/a = 0.6$.

With this choice of parameters and profiles, the most unstable mode for the electrostatic case $(\beta_e = 0)$ should be an ion-temperature-gradient-driven (ITG) mode, driven by the interplay between the magnetic drifts of the plasma particles and the background temperature gradient. The code recovers this result. For the case of $\beta_e = 1\%$, the dominant mode is still an ITG mode partially stabilized by finite β_e effects. For $\beta_e > 2\%$, the most unstable mode is an EM kinetic ballooning mode (see Figs. 2 and 3). Note that only the mode with toroidal mode

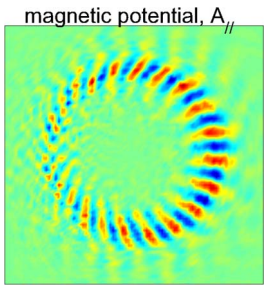

Fig. 4. Linear ORB5 simulations: Typical example of a poloidal cross section of the parallel magnetic potential, $A_{\parallel}$ ($\beta_e = 2\%$).

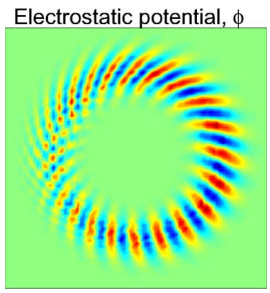

Fig. 5. Linear ORB5 simulations: Typical example of a poloidal cross section of the electrostatic potential, φ ($\beta_e = 2\%$).

number $n = 12$ has been kept in the simulation. A similar set of parameters and profiles has been used in the β_e scan presented in [16, Fig. 11] with the linear code GYGLES. In this case, the ORB5 and GYGLES results are in good qualitative and quantitative agreement. Figs. 4 and 5 show the spatial structure of the electrostatic and magnetic potentials in the tokamak cross section for a typical case. Both fields show the ballooning structures and the presence of rational surfaces as already seen in the other global linear simulations (see, for example, [20]). The nonlinear simulations of Fig. 6 are based on the parameters and profiles of the Cyclone base case, described in [12], and are already used for the strong scaling of Fig. 1. The mass ratio is $m_i/m_e = 1000$, and the value of the central density has been adjusted to have $\beta_e = 0.3\%$. Note that, in these simulations (as well as in [12]), no heat sources are applied, and the initial temperature gradient ($R/L_T \simeq 10$) relaxes during the time evolution toward the critical gradient value. The EM simulation was performed using 512 million numerical particles per species and with a time step 20 times smaller than the electrostatic case ($\Delta t = 1\ \Omega_i$, where Ω_i is the ion cyclotron frequency). The radial resolution (512 grid points) is four times higher than that in the electrostatic simulations (128 grid points). The initial nonlinear EM ORB5 simulations demonstrated that such high radial resolutions are required to describe the nonadiabatic electron dynamics in the vicinity of resonant surfaces. When the radial resolution is too poor, spurious modes appear in the EM simulations [22], which are not present in the electrostatic simulations with adiabatic electrons. The dissipation necessary to assure entropy saturation is provided by a residual zonal flow conserving the noise-control algorithm [11], [21]. Fig. 6 compares the time evolution of the ion thermal diffusivity of a $\beta = 0.3\%$ EM simulation (red) with that of one of the original electrostatic simulation of [12]. The ion thermal diffusivity is

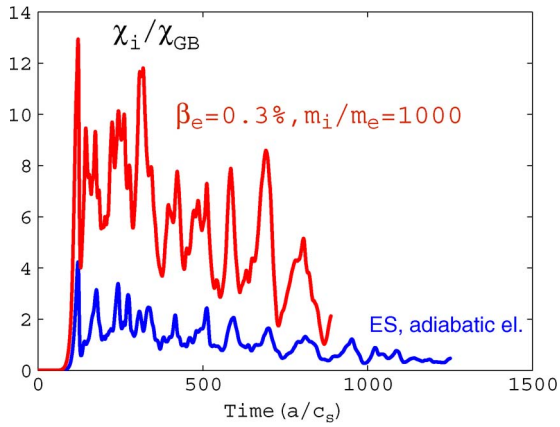

Fig. 6. Time evolution of the ion thermal diffusivity for (red) an EM $\beta_e = 0.3\%$ simulation and the standard electrostatic Cyclone case.

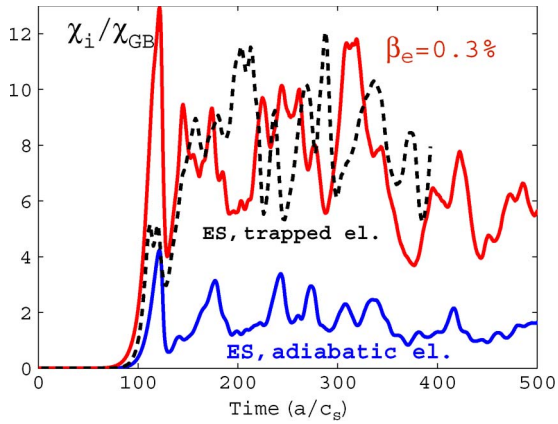

Fig. 7. Time evolution of the ion thermal diffusivity for (red) an EM $\beta_e = 0.3\%$ simulation and electrostatic simulation (black and dashed) with and (blue) without trapped electrons.

clearly larger in the $\beta_e = 0.3\%$ simulation as compared to that in the reference benchmark case. It is important to notice that, in the reference benchmark simulations, the electrons are assumed to be adiabatic. The trapped electron dynamics, present in the EM simulation but absent in the benchmark case, contributes to further destabilize the ITG instability (see, for example, [23]). We have performed an additional electrostatic simulation considering the gyrokinetic ions, adiabatic passing electrons, and drift-kinetic trapped electrons, following the numerical scheme described in [24] and [25]. Fig. 7 shows that the ion thermal diffusivity for the electrostatic simulation, including the trapped electrons, is comparable with that of the EM case. A detailed analysis of the heat fluxes shows that, in the $\beta = 0.3\%$ case, the magnetic flutter terms are almost two orders of magnitude smaller than the electrostatic contribution and do not affect the ions, which is in agreement with the existing flux-tube results [26]–[28]. During the simulation, the signal/noise diagnostics [29] gives a noise/signal ratio ranging between 5% and 10%.

Fig. 8 shows the spectrum of the electrostatic and EM potentials at the end of the simulation. Both $A_{\parallel}^2$ and ϕ^2 spectra reach a maximum for the same value of toroidal mode number and show an identical power-law decay behavior for a high n. The same result is present in gyrofluid simulations. An example is given in Fig. 9, obtained with the GEMR [30] code, where

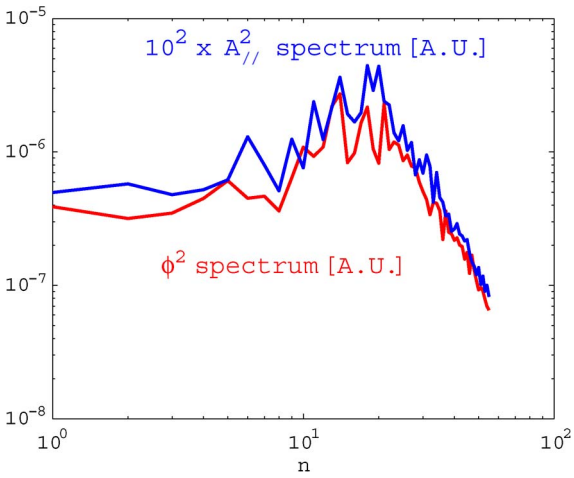

Fig. 8. Spectrum of the potential fields at $t \simeq 800\ [a/c_s]$ as a function of the toroidal mode number n.

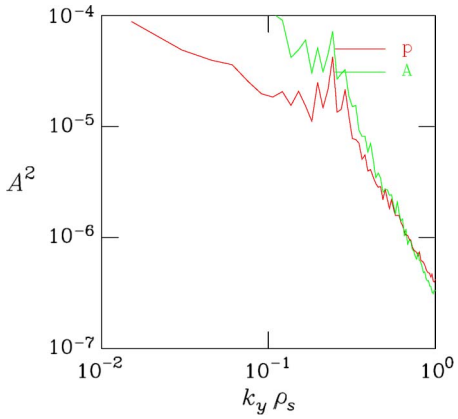

Fig. 9. Spectrum of the potential fields (p in the figure) ϕ^2 and (A in the figure) $\beta_e A_\parallel^2$ for $\beta_e = 0.4\%$ obtained with the gyrofluid code GEMR [30]. Normalization: $\phi[T_e/e]A_\parallel[B\rho_s\beta_e]$.

the $A_\parallel^2$ and ϕ^2 spectra are plotted as a function of $k_y\rho_s \propto n$. The main difference between the gyrofluid and gyrokinetic spectra appears at low n values, where the GEMR values are significantly higher than the ORB5 ones. Note that the GEMR code does not include the trapped electron dynamics.

V. Conclusion

In this paper, we have presented the first global nonlinear EM simulations of the finite β_e effects in the tokamak geometry. The parallel component of Ampère's law has been successfully added in the code ORB5, and we have proven that the adjustable control variate method of [6] can be used to solve the cancellation problem in the nonlinear simulations. Many improvements in the algorithm are still possible; in particular, an iterative procedure can be added to the adjustable control variate method (see [6] and [19]). This iterative algorithm has been implemented in the ORB5, and it is now under testing. It is important to underline that, even using all the control techniques available, the achievement of converged global nonlinear EM simulations requires a larger amount of numerical resources than the standard electrostatic simulations with adiabatic electrons. This is mainly due to the constraints imposed by the interplay of the Alfvén dynamics and kinetic electrons which requires smaller time steps, finer spatial discretization, and, consequently, a higher number of markers.

Acknowledgment

All the simulations presented in this paper were performed on the IBM BlueGene/P and IBM POWER6 computers of Rechenzentrum Garching of the Max Planck Society and the IPP and on the EFDA HPC-FF parallel computer under the NEMORB5 project.

References

[1] W. W. Lee, "Gyrokinetic approach in particle simulation," *Phys. Fluids*, vol. 26, no. 2, pp. 556–562, Feb. 1983.
[2] W. W. Lee, "Gyrokinetic particle simulation model," *J. Comput. Phys.*, vol. 72, p. 243, 1987.
[3] S. E. Parker and W. W. Lee, "A fully nonlinear characteristic method for gyrokinetic simulation," *Phys. Fluids B*, vol. 5, no. 1, pp. 77–86, Jan. 1993.
[4] A. M. Dimits and W. W. Lee, "Partially linearized algorithms in gyrokinetic particle simulation," *J. Comput. Phys.*, vol. 107, no. 2, pp. 309–323, Aug. 1993.
[5] A. Y. Aydemir, "A unified Monte Carlo interpretation of particle simulations and applications to non neutral plasmas," *Phys. Plasmas*, vol. 1, p. 822, 1994.
[6] R. Hatzky, A. Könies, and A. Mishchenko, "Electromagnetic gyrokinetic PIC simulation with an adjustable control variates method," *J. Comput. Phys.*, vol. 225, no. 1, pp. 568–590, Jul. 2007.
[7] F. Zonca, L. Chen, J. Q. Dong, and R. A. Santoro, "Existence of ion temperature gradient driven shear Alfvén instabilities in tokamaks," *Phys. Plasmas*, vol. 6, no. 5, pp. 1917–1924, May 1999.
[8] Y. Chen and S. Parker, "A δf particle method for gyrokinetic simulations with kinetic electrons and electromagnetic perturbations," *J. Comput. Phys.*, vol. 189, no. 2, pp. 463–475, Aug. 2003.
[9] A. Mishchenko, R. Hatzky, and A. Könis, "Conventional δf-particle simulations of electromagnetic perturbations with finite elements," *Phys. Plasmas*, vol. 11, no. 12, pp. 5480–5486, Dec. 2004.
[10] S. Jolliet, A. Bottino, P. Angelino, R. Hatzky, T. M. Tran, B. F. Mcmillan, O. Sauter, K. Appert, Y. Idomura, and L. Villard, "A global collisionless PIC code in magnetic coordinates," *Comput. Phys. Commun.*, vol. 177, no. 5, pp. 409–425, Sep. 2007.
[11] B. F. McMillan, S. Jolliet, T. M. Tran, A. Bottino, L. Villard, and P. Angelino, "Avalanchelike bursts in global gyrokinetic simulations," *Phys. Plasmas*, vol. 16, no. 2, p. 022 310, Feb. 2009.
[12] G. L. Falchetto, B. D. Scott, P. Angelino, A. Bottino, T. Dannert, V. Grandgirard, S. Janhunen, F. Jenko, S. Jolliet, A. Kendl, B. F. McMillan, V. Naulin, A. H. Nielsen, M. Ottaviani, A. G. Peeters, M. J. Pueschel, D. Reiser, T. T. Ribeiro, and M. Romanelli, "The European turbulence code benchmarking effort: Turbulence driven by thermal gradients in magnetically confined plasmas," *Plasma Phys. Control. Fusion*, vol. 50, no. 12, p. 124 015, Dec. 2008.
[13] [Online]. Available: www.efda-itm.eu
[14] T. S. Hahm, W. W. Lee, and A. Brizard, "Nonlinear gyrokinetic theory for finite-beta plasmas," *Phys. Fluids*, vol. 31, no. 7, pp. 1940–1948, Jul. 1988.
[15] T. S. Hahm, "Nonlinear gyrokinetic equations for tokamak microturbulence," *Phys. Fluids*, vol. 31, no. 9, pp. 2670–2673, Sep. 1988.
[16] A. Brizard, "Nonlinear gyrokinetic Maxwell-Vlasov equations using magnetic co-ordinates," *J. Plasma Phys.*, vol. 41, no. 3, pp. 541–559, Jun. 1989.
[17] H. Lütjens, A. Bondeson, and O. Sauter, "The CHEASE code for toroidal MHD equilibria," *Comput. Phys. Commun.*, vol. 97, no. 3, pp. 219–260, Sep. 1996.
[18] K. Höllig, *Finite Elements Methods With B-Splines*. Philadelphia, PA: SIAM, 2003.
[19] A. Mishchenko, R. Hatzky, and A. Könis, "Global particle-in-cell simulations of Alfvénic modes," *Phys. Plasmas*, vol. 15, no. 11, p. 112 106, Nov. 2008.

[20] G. L. Falchetto, J. Vaclavik, and L. Villard, "Global-gyrokinetic study of finite β effects on linear microinstabilities," *Phys. Plasmas*, vol. 10, no. 5, pp. 1424–1436, May 2003.
[21] S. Jolliet, B. F. McMillan, T. Vernay, L. Villard, A. Bottino, and P. Angelino, "Quasisteady and steady states in global gyrokinetic particle-in-cell simulations," *Phys. Plasmas*, vol. 16, no. 5, p. 052 307, May 2009.
[22] B. Scott, "Computation of turbulence in magnetically confined plasmas," *Plasma Phys. Control. Fusion*, vol. 48, no. 12B, pp. B277–B293, Dec. 2006.
[23] L. Villard, A. Bottino, O. Sauter, and J. Vaclavik, "Radial electric fields and global electrostatic microinstabilities in tokamaks and stellarators," *Phys. Plasmas*, vol. 9, no. 6, pp. 2684–2691, Jun. 2002.
[24] S. Jolliet, "Gyrokinetic particle-in-cell global simulations of ion-temperature-gradient and collisionless-trapped-electron-mode turbulence in tokamaks," Ph.D. dissertation, no 4326, Ecole Polytechnique Fédérale de Lausanne, Lausanne, Switzerland, 2009.
[25] A. Bottino, A. G. Peeters, O. Sauter, J. Vaclavik, and L. Villard, "Simulations of global electrostatic microinstabilities in ASDEX Upgrade discharges," *Phys. Plasmas*, vol. 11, no. 1, pp. 198–206, Jan. 2004.
[26] R. E. Waltz, "Numerical simulation of electromagnetic turbulence in tokamaks," *Phys. Fluids*, vol. 28, no. 2, pp. 577–589, Feb. 1985.
[27] B. Scott, "Three-dimensional computation of drift Alfvén turbulence," *Plasma Phys. Control. Fusion*, vol. 39, no. 10, pp. 1635–1668, Oct. 1997.
[28] J. Candy, "Beta scaling of transport in microturbulence simulations," *Phys. Plasmas*, vol. 12, no. 7, p. 072 307, Jul. 2005.
[29] A. Bottino, A. G. Peeters, R. Hatzky, S. Jolliet, B. F. McMillan, T. M. Tran, and L. Villard, "Nonlinear low noise particle-in-cell simulations of electron temperature gradient driven turbulence," *Phys. Plasmas*, vol. 14, no. 1, p. 010 701, Jan. 2007.
[30] B. Scott, "Free-energy conservation in local gyrofluid models," *Phys. Plasmas*, vol. 12, no. 10, p. 102 307, Oct. 2005.

Alberto Bottino received the Ph.D. degree from Ecole Polytechnique Fédérale de Lausanne, Lausanne, Switzerland, in 2004.

Since 2006, he has been with the turbulence group of the theory division of Max-Planck-Institut für Plasmaphysik, Garching, Germany. His research interests include the numerical simulation of plasma turbulence using particle-in-cell algorithms.

Bruce Scott received the Ph.D. degree from the University of Maryland, College Park, in 1985.

Since 1988, he has been with the Max-Planck-Institut für Plasmaphysik, Garching, Germany. He is active in the field of magnetized plasma physics for over 25 years with over 60 published papers.

Stephan Brunner received the Ph.D. degree in physics from the Ecole Polytechnique Fédérale de Lausanne (EPFL), Lausanne, Switzerland, in 1998, where he worked on the study of microinstabilities in magnetized plasmas.

He was with the theory group at PPPL for three years, where he carried out research related to laser plasma interaction. For two additional years in the industry, he developed numerical simulation tools for molecular modeling. Since 2003, he has been with the CRPP, EPFL. His current main research interests include the development and application of Eulerian and PIC codes for studying the kinetic effects in magnetic and inertial fusion relevant plasmas.

Ben F. McMillan received the Ph.D. degree from The Australian National University, Canberra, Australia.

He works in gyrokinetic microturbulence and studies the numerical issues and dynamical behavior of these complex nonlinear systems.

Trach Minh Tran received the Ph.D. degree in physics from the Ecole Polytechnique Fédérale de Lausanne (EPFL), Lausanne, Switzerland, in 1983.

He is currently with the Centre de Recherches en Physique des Plasmas, EPFL, where he is working on high-power RF sources and gyrokinetic microturbulence simulations.

Thibaut Vernay received the M.S. degree in physics from the Ecole Polytechnique Fédérale de Lausanne (EPFL), Lausanne, Switzerland, in 2008. He is currently working toward the Ph.D. degree in the Centre de Recherches en Physique des Plasmas, EPFL, where he is working on the gyrokinetic code ORB5.

Laurent Villard obtained the Ph.D. degree in physics from the Ecole Polytechnique Fédérale de Lausanne (EPFL), Lausanne, Switzerland, in 1987, where he worked on the numerical simulation of RF waves using a finite-element method.

For three years, he was on various teaching assignments abroad. He is currently with the Centre de Recherches en Physique des Plasmas, EPFL, where he is conducting research on macroscopic stability and kinetic interactions with fast ions. His current research interests include the first-principle-based numerical simulations of turbulence in magnetically confined plasmas using the gyrokinetic theory and implying massively parallel algorithms.

Sebastien Jolliet received the Ph.D. degree from Ecole Polytechnique Fédérale de Lausanne, Lausanne, Switzerland, in 2009.

He is currently with the Japan Atomic Energy Agency, Tokyo, Japan. He is working in the field of gyrokinetics and has contributed to the development of the particle-in-cell code ORB5 and the Eulerian code GT5D.

Roman Hatzky received the Ph.D. degree from Christian-Albrechts-University Kiel, Kiel, Germany, in 1996.

Since 2000, he has been with the Max-Planck-Institut für Plasmaphysik, Garching, Germany, as a member of the research staff.

Arthur G. Peeters obtained the Ph.D. degree from Eindhoven Technical University, Eindhoven, The Netherlands, in 1994.

From 1995 to 2006, he was with the Max-Planck-Institut für Plasmaphysik, Garching, Germany. Since 2006, he has been with the University of Warwick, Coventry, U.K., where he was appointed as a Full Professor in 2009. Since June 2010, he has been a Lichtenberg Professor with the University of Bayreuth, Bayreuth, Germany.